Proteomic Analysis of Protein Expression and Oxidative Modification in R6/2 Transgenic Mice

A MODEL OF HUNTINGTON DISEASE*

Marzia Perluigi,[a,b] H. Fai Poon,[b] William Maragos,[c,d] William M. Pierce,[e] Jon B. Klein,[f] Vittorio Calabrese,[g] Chiara Cini,[a] Carlo De Marco,[a] and D. Allan Butterfield[b,h,i,j]

Huntington disease (HD) is a hereditary neurodegenerative disorder characterized by motor, psychiatric, and cognitive symptoms. The genetic defect responsible for the onset of the disease, expansion of CAG repeats in exon 1 of the gene that codes for huntingtin on chromosome 4, has been unambiguously identified. On the other hand, the mechanisms by which the mutation causes the disease are not completely understood yet. However, defects in energy metabolism of affected cells may cause oxidative damage, which has been proposed as one of the underlying molecular mechanisms that participate in the etiology of the disease. In our effort to investigate the extent of oxidative damage occurring at the protein level, we used a parallel proteomic approach to identify proteins potentially involved in processes upstream or downstream of the disease-causing huntingtin in a well established HD mouse model (R6/2 transgenic mice). We have demonstrated that the expression levels of dihydrolipoamide *S*-succinyltransferase and aspartate aminotransferase increase consistently over the course of disease (10-week-old mice). In contrast, pyruvate dehydrogenase expression levels were found to be decreased in 10-week-old HD transgenic mice compared with young (4-week-old) mice. Our experimental approach also led to the identification of oxidatively modified proteins. Six proteins were found to be significantly oxidized in old R6/2 transgenic mice compared with either young transgenic mice or non-transgenic mice. These proteins are α-enolase, γ-enolase (neuron-specific enolase), aconitase, the voltage-dependent anion channel 1, heat shock protein 90, and creatine kinase. Because oxidative damage has proved to play an important role in the pathogenesis and the progression of Huntington disease, our results for the first time identify specific oxidatively modified proteins that potentially contribute to the pathogenesis of Huntington disease. *Molecular & Cellular Proteomics 4: 1849–1861, 2005.*

Huntington disease (HD)[1] is a progressive autosomal dominant disorder caused by an expanded CAG repeat in exon 1 of the *huntingtin* gene located on chromosome 4. Clinical symptoms of HD generally include psychiatric abnormalities, most commonly depression and mood disturbances, which typically manifest in midlife, and involuntary choreiform movements and dementia develop over a period of 15–20 years. Death generally results from complications of immobility (1). Neuropathologically the disease is characterized by bilateral striatal atrophy with marked neuronal loss and astrogliosis within the caudate and putamen.

The HD gene mutation is an expansion of a trinucleotide CAG repeat that encodes the non-essential amino acid glutamine in a coding region of about 350 kb. The normal range for the number of glutamines in the polyglutamine tract is between 6 and 34 with disease being found when the polyglutamine tract is greater than 40. The age of onset and the severity of the disease are correlated with the length of the CAG expansion (2, 3). A direct causative pathway from the HD gene mutation to neuronal dysfunction and death has not yet been established. In HD, both normal and mutant alleles are expressed. Gain of function alterations in which mutant huntingtin has toxicity as well as loss of function of normal huntingtin have been proposed to contribute to HD pathogenesis (4). The elucidation of a pathogenic function for mutant huntingtin is currently the subject of intense research activity, but little is known about its potential roles in cell death processes, and tissue distribution studies give little insight into the re-

[1] The abbreviations used are: HD, Huntington disease; AD, Alzheimer disease; ALS, amyotrophic lateral sclerosis; ROS, reactive oxygen species; 2D, two-dimensional; DNP, 2,4-dinitrophenylhydrazone; VDAC-1, voltage-dependent anion channel 1; HSP, heat shock protein; CTR, control; CK, creatine kinase; MtCK, mitochondrial CK; NSE, neuron-specific enolase; E2, dihydrolipoamide *S*-succinyltransferase; E1, 2-oxoglutarate dehydrogenase; E3, lipoamide dehydrogenase; PDHC, pyruvate dehydrogenase; PTP, permeability transition pore.

gional selectivity of cell loss in the disease. The pathogenetic mechanisms in HD are far from understood but have been suggested to involve altered mitochondrial mechanism, excitotoxicity, oxidative stress, and possibly an impairment of the ubiquitin proteasome system (1, 5).

Like other age-dependent neurodegenerative diseases, including Alzheimer disease (AD), Parkinson disease, amyotrophic lateral sclerosis (ALS), and prion disease, HD is also a protein misfolding disease. The hallmark of mutant huntingtin is the formation of intranuclear inclusions and cytoplasmic aggregates in neurons in vulnerable brain areas. The inclusions and aggregates are usually formed by small N-terminal fragments and are co-localized with other cellular proteins involved in proteolysis, vesicle trafficking, and protein degradation.

Recently growing interest has been focused on the role of oxidative stress in the pathogenesis of HD, and a number of studies indicate increased levels of oxidative damage in HD brains (1). These oxidative modifications include increased incidence of DNA strand breaks (6), exacerbated lipofuscin accumulation (7), and increased immunohistochemical staining of oxidatively damaged products in HD striatum and cortex (1). Indeed HD is postulated to involve a mitochondrial metabolic defect (8), and strong evidence from several laboratories supports this view (1, 9, 10). Energetic defects might occur as a primary event in HD or as a consequence of oxidative damage to cellular elements. Reduced ATP production due to impaired mitochondrial energy metabolism can result in partial cell depolarization by making neurons more vulnerable to endogenous levels of glutamate (11, 12). The concomitant increase of Ca^{+2} influx into neurons may trigger further free radical production, exacerbating damage to cellular elements (13). Free radicals can induce oxidative damage to cell macromolecules including DNA, proteins, and lipids by a number of different mechanisms such as formation of DNA adducts, protein carbonylation, and lipid peroxidation (14–16).

Oxidative damage of proteins is one of the modifications leading to a severe failure of biological functions and to cell death. However, oxidative stress is also an inevitable part of normal metabolism in an aerobic environment in which reactive oxygen species (ROS) are generated. ROS may oxidize amino acid residue side chains into ketone or aldehyde derivatives (17). Histidine, arginine, and lysine are the most susceptible amino acids for the ROS-mediated carbonyl formation (18). Measurement of these carbonyl groups is thought to be a good estimation for the extent of oxidative damage of proteins associated with various conditions of oxidative stress, aging, physiological disorders, and diseases (19, 20).

An important advance in the study of HD was the development of transgenic mouse models. The R6/2 mouse, which expresses exon 1 of the human HD gene with an expanded CAG trinucleotide repeat (around 150 CAG repeats), is the most widely studied HD model system (21). This model exhibits decreased striatal and total brain size, ubiquitinated

nuclear and cytoplasmic inclusion bodies, altered levels of neurotransmitters and their receptors, decreased expression of striatal signaling genes, and progressive motor and cognitive deficits (22, 23). The degree to which R6/2 animals have been characterized combined with their relatively consistent time line of biochemical and behavioral changes provides an opportunity to determine where a particular biochemical component falls within the cascade of the disease process. To investigate the role of oxidative stress in the etiology of selective neuronal death in HD, we used a parallel proteomic approach to identify striatal proteins differentially expressed and oxidatively modified in R6/2 transgenic mice.

MATERIALS AND METHODS

Animals and Tissue—Transgenic HD mice of the R6/2 strain and littermate controls were obtained according to the protocol from The Jackson Laboratory (Bar Harbor, ME). Male R6/2 mice were bred with females from their background strain (B6CBAFI/J). The offspring were genotyped by PCR assay of DNA obtained from tail tissue. CAG repeat length was examined to ensure that a drift in number of CAG repeats did not play a role in the outcome of the studies. Mice were housed with a 12-h light-dark cycle, and animals were given free access to food and water. All experiments were conducted after institutional approval of the animal use subcommittee, which subscribes to the National Institutes of Health Guide for Care and Use of Laboratory Animals. Brains of 4- and 10-week-old R6/2 transgenic mice as well as control mouse brains were used in our studies. Methods to kill the animals were approved and involved no or only transiently minimal pain.

Sample Preparation—Six 4-week-old and six 10-week-old R6/2 transgenic mice brains as well as control mouse brains were flash frozen in liquid nitrogen after dissection. Tissue samples from striatum were homogenized by suspending in 10 mM HEPES containing 137 mM NaCl, 4.6 mM KCl, 1.1 mM KH_2PO_4, and the following proteinase inhibitors: leupeptin (0.5 mg/ml), pepstatin (0.7 μg/ml), type IIS soybean trypsin inhibitor (0.5 μg/ml), and PMSF (40 μg/ml). Homogenates were sonicated for 20 s three times and then centrifuged at 14,000 × g for 15 min to remove debris. Protein concentration in the supernatant was assayed by the BCA method (Pierce).

Two-dimensional Gel Electrophoresis—Protein samples from striatum were prepared according to the procedure of Levine *et al.* (24). 100 μg of protein were incubated with 4 volumes of 2 N HCl at room temperature (25 °C) for 20 min. Proteins were then precipitated by addition of ice-cold 100% TCA to obtain a final concentration of 15% TCA. Samples were placed on ice for 10 min to allow precipitation of proteins. Precipitates were centrifuged at 15,800 × g for 2 min. The pellets were washed with 0.5 ml of 1:1 (v/v) ethanol/ethyl acetate solution. After centrifugation and washing with ethanol/ethyl acetate solution three times, the samples were dissolved in 25 μl of 8 M urea (Bio-Rad). The samples were then mixed with 185 μl of rehydration buffer (8 M urea, 20 mM dithiothreitol, 2.0% (w/v) CHAPS, 0.2% Biolytes, 2 M thiourea, and bromphenol blue).

For the first-dimension electrophoresis, 200 μl of sample solution were applied to a ReadyStrip™ IPG® strip, pH 3–10 (Bio-Rad). The strips were soaked in the sample solution for 1 h to allow uptake of the proteins. The strip was then actively rehydrated in a Protean IEF cell (Bio-Rad) for 16 h at 50 V. The isoelectric focusing was at 300 V for 2 h linearly, 500 V for 2 h linearly, 1000 V for 2 h linearly, 8000 V for 8 h linearly, and 8000 V for 10 h rapidly. All the processes above were carried out at 22 °C. The focused IEF strip was stored at −80 °C until second dimension electrophoresis was performed.

For second dimension electrophoresis, thawed IPG strips were equilibrated for 10 min in 50 mM Tris-HCl (pH 8.8) containing 6 M urea,

1% (w/v) SDS, 30% (v/v) glycerol, and 0.5% dithiothreitol and then re-equilibrated for 15 min in the same buffer containing 4.5% iodoacetamide in place of dithiothreitol. Proteins were then separated according to their M_r on 8–16% SDS-PAGE using precast Criterion Tris-HCl gels (Bio-Rad) to perform second dimension electrophoresis. Precision Protein™ standards (Bio-Rad) were run along with the sample at 200 V for 65 min.

At the end of the run gels were incubated in fixing solution (7% acetic acid, 10% methanol) for 20 min. Approximately 40 ml of SYPRO Ruby gel stain (Bio-Rad) were used to stain the gels for 2 h on a gently continuous rocker. The gels were placed in deionized water overnight for destaining.

Western Blotting—The same amount of protein samples (100 μg) was used for detecting specific protein carbonyl levels, and the electrophoresis was carried out in the same way as described above. 100 μg of proteins were incubated with 4 volumes of 20 mM 2,4-dinitrophenylhydrazine at room temperature (25 °C) for 20 min. The gels were prepared in the same manner as 2D electrophoresis. The proteins from the second dimension electrophoresis gels were transferred to nitrocellulose (Bio-Rad) using a Transblot-Blot® SD semidry transfer cell (Bio-Rad) at 15 V for 2 h. The 2,4-dinitrophenylhydrazone (DNP) adducts of the carbonyls of the proteins were detected on the nitrocellulose paper using a primary rabbit antibody (Intergen) specific for DNP-protein adduct (1:100) followed by a secondary goat anti-rabbit IgG (Sigma**)** antibody. The resultant stain was developed using 5-bromo-4-chloro-3-indolyl phosphate/nitro blue tetrazolium solution (SigmaFast tablets, Sigma).

Image Analysis—The two-dimensional gels (six for each of the following groups: 4- and 10-week-old R6/2 transgenic mice and 4- and 10-week old non-transgenic mice, a total of 24 gels), and two-dimensional nitrocellulose blots (six Western blots for each group, total $n = 24$ blots) were scanned and saved in TIF format using a Scanjet 3300C (Hewlett Packard). PDQuest 2D analysis software (Bio-Rad) was used for matching and analysis of visualized protein spots among differential gels and membranes to compare protein and DNP immunoreactivity content between R6/2 transgenic and non-transgenic mice (4- and 10-week-old mice). This sophisticated software offers powerful comparative analysis and is specifically designed to analyze many gels or blots at once. Powerful automatching algorithms quickly and accurately assist matching gels or blots, and sophisticated statistical analysis tools allow identification of experimentally significant spots. The principles of measuring intensity values by 2D analysis software were similar to those of densitometric measurement. The average mode of background subtraction was used to normalize intensity values, which represents the amount of protein (total protein on gel and DNP-protein adduct on the membrane) per spot. After completion of spot matching, the normalized intensity of each protein spot from individual gels (or membranes) was compared between groups using statistical analysis. Statistical significance was assessed by a two-tailed Student's t test. p values <0.05 were considered significant for comparison between control (non-transgenic mice) and experimental data (R6/2 transgenic mice). Trypsin digestion was only preformed on the spots that are considered significant by Student's t test analysis.

Trypsin Digestion—In-gel digestion on selected gel spots was performed according to Thongboonkerd *et al.* (25). The selected protein spots, excised with a blade and transferred into microcentrifuge tubes, were washed with 0.1 M ammonium bicarbonate (NH_4HCO_3) at room temperature for 15 min. A second wash was performed using acetonitrile for 15 min at room temperature. The solvent was removed, and the gel pieces were dried in a flow hood. The protein spots were incubated with 20 μl of 20 mM DTT in 0.1 M NH_4HCO_3 at 56 °C for 45 min. The DTT solution was then removed and replaced with 20 μl of 55 mM iodoacetamide in 0.1 M NH_4HCO_3. The solution

was incubated at room temperature in the dark for 30 min. The iodoacetamide was removed and replaced with 0.2 ml of 50 mM NH_4HCO_3 and incubated at room temperature for 15 min. 200 μl of acetonitrile was added. After a 15-min incubation, the solvent was removed, and the gel spots were dried in a flow hood for 30 min. The gel pieces were rehydrated with 20 ng/μl methylated trypsin (Promega, Madison, WI) in 50 mM NH_4HCO_3 with the minimal volume to cover the gel pieces. The gel pieces were chopped into smaller pieces and incubated at 37 °C overnight in shaking incubator.

Mass Spectrometry—All mass spectra reported in this study were acquired using a Spec 2E MALDI-TOF mass spectrometer operated in the reflectron mode to generate peptide mass fingerprints. Peptides resulting from in-gel digestion with trypsin were analyzed on a 384-position, 600-μm AnchorChip™ target (Bruker Daltonics, Bremen, Germany) and prepared according to AnchorChip recommendations (AnchorChip Technology, Revision 2, Bruker Daltonics). Briefly 1 μl of digest was mixed with 1 μl of aα-cyano-4-hydoxycinnamic acid (0.3 mg/ml in ethanol/acetone, 2:1 ratio) directly on the target and allowed to dry at room temperature. The sample spot was washed with 1 μl of a 1% TFA solution for ∼60 s. The TFA droplet was gently blown off the sample spot with compressed air. The resulting diffuse sample spot was recrystallized (refocused) using 1 μl of a solution of ethanol/acetone/0.1% TFA (6:3:1 ratio). Spectra were obtained as a summation of 100 laser shots. External calibration of the mass axis was used for acquisition, and internal calibration using either trypsin autolysis ions or matrix clusters was applied postacquisition for accurate mass determination.

The MALDI spectra used for protein identification from tryptic fragments were searched against the National Center for Biotechnology Information (NCBI) protein databases using the MASCOT search engine (www.matrixscience.com). Peptide mass fingerprinting used the assumption that peptides are monoisotopic, oxidized at methionine residues, and carbamidomethylated at cysteine residues (26). Up to one missed trypsin cleavage was allowed. A mass tolerance of 150 ppm was the window of error allowed for matching the peptide mass values. Probability-based MOWSE scores were estimated by comparison of search results against estimated random match population and were reported as $-10 \times \log_{10}(p)$ where p is the absolute probability. MOWSE scores greater than 61 were considered significant. All the protein identifications were in the expected size range based on position in the gel.

Immunoprecipitation—Immunoprecipitation was performed essentially as described previously (27). A mouse anti-heat shock protein 90 antibody (10 μl) (Sigma) or a rabbit anti-voltage-dependent anion channel 1 (VDAC-1) antibody (10 μl) (Sigma) was added directly to the brain homogenate. Antibody/lysate solutions were incubated on a rotary mixer overnight at 4 °C. The antigen-antibody complexes were precipitated with protein A-conjugated (for rabbit antibody) or protein G-conjugated (for mouse antibody) agarose beads. Protein A beads or protein G beads were added in 50-μl aliquots from a stock of 300 mg/ml in PBS and mixed on a rotary mixer for 1 h at room temperature. Beads were then centrifuged, and 2D electrophoresis was performed on the supernatant.

Creatine Kinase Activity— Creatine kinase activity was performed using a commercial kit (Stanbio Laboratory). Briefly 75 μl of substrate solution (2 mM ADP, 5 mM AMP, 10 mM diadenosine pentaphosphate, 2 mM NAD, 3000 units/liter hexokinase, 3000 units/liter glucose-6-phosphate dehydrogenase, 20 mM *N*-acetylcysteine, 30 mM creatine phosphate, 20 mM D-glucose, 10 mM Mg^{2+}, 2 mM EDTA) were mixed with 10 μl of brain homogenate. The enzymatic activity was determined by the change of absorption at A_{340} for 10 min.

Enolase Activity—The enolase activity assay was performed as described previously (28) with minor modifications (29). 10 μl of brain homogenates were added to 100 μl of assay mixture (20 mM
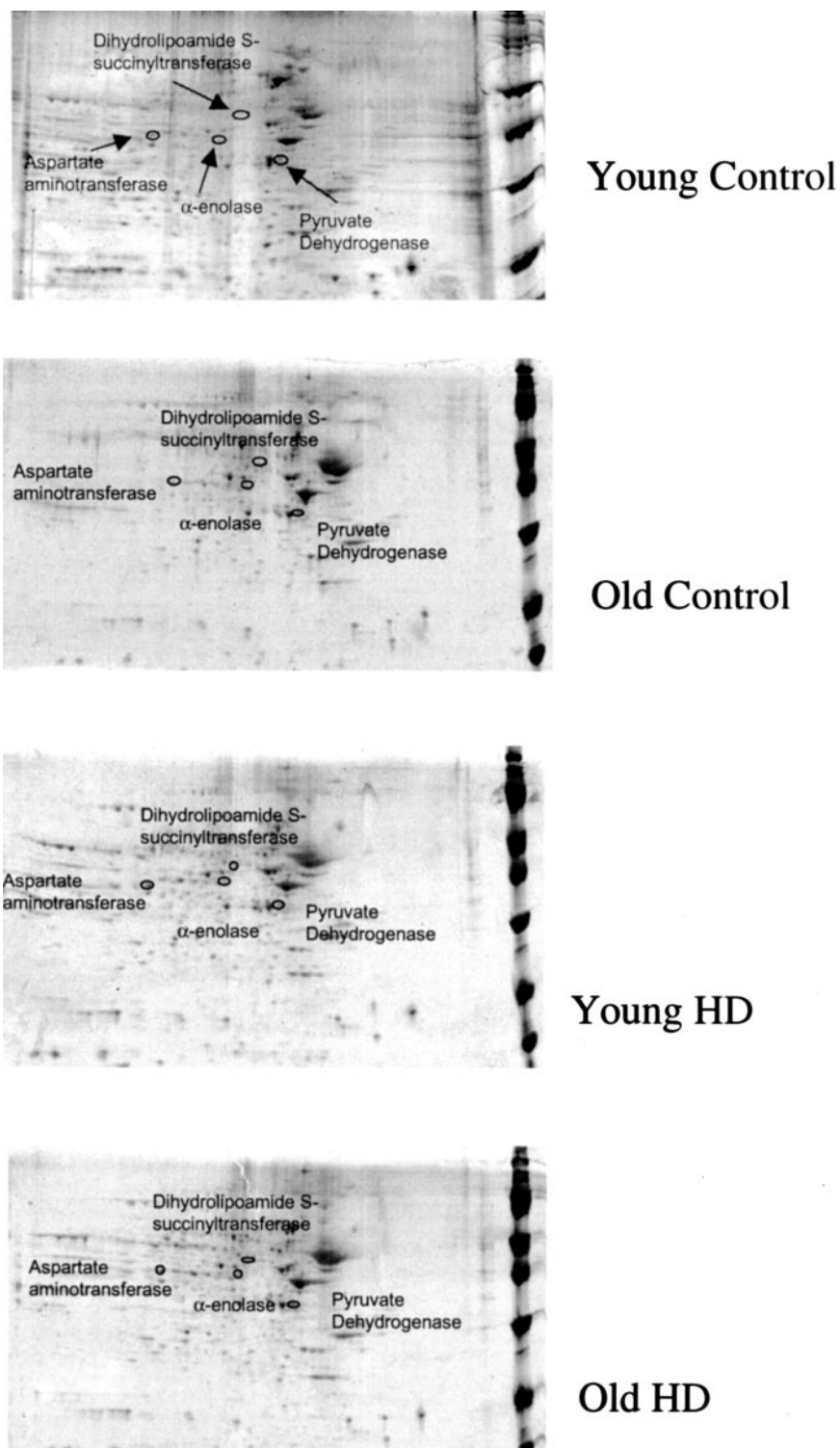
FIG. 1. **Two-dimensional SYPRO Ruby-stained gel from R6/2 transgenic mice (*Young* and *Old HD*) and non-transgenic mice (*Young* and *Old Control*).** Positions of the identified proteins are shown on the gels. Expanded images of the identified spots are also shown. *Young*, 4-week-old mice; *Old*, 10-week-old mice.

Na_2HPO_4, pH 7.4, 400 mM KCl, 0.01 mM EDTA, 2 mM 2-phospho-D-glycerate) in a UV light-transparent microtiter plate (Corning). The enzymatic activity was determined by the change of absorption at A_{240} for 5 min.

Proteomic Data Analysis—The interactions of proteins that show altered expression and oxidation in R6/2 mice were analyzed using Interaction Explorer™ Software PathwayAssist (Stratagene). The interactions between the proteins of interest were searched in a database of over 500,000 biological interactions built by applying the MedScan text-mining algorithms to all PubMed abstracts. These interactions were then visualized in an interaction network.
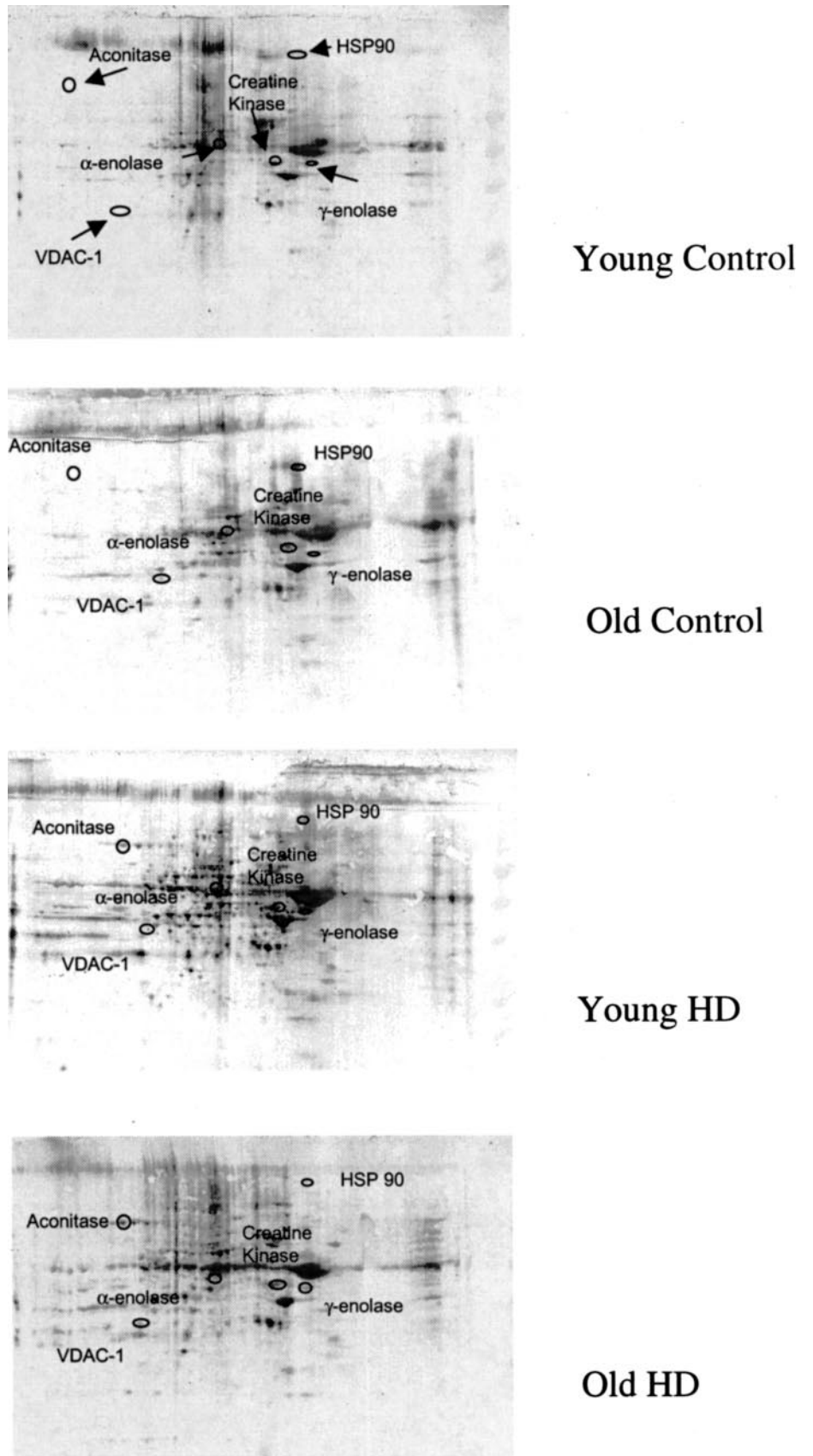
FIG. 2. **Carbonyl immunoblot from 10-week-old (*Old*) and 4-week-old (*Young*) R6/2 transgenic mice and non-transgenic mice (*Control*).**

TABLE I
Summary of the proteins identified by proteomic analysis

Identified protein	Percent coverage matched peptides	pI, molecular mass	MOWSE score	Probability of a random identification
		kDa		
α-Enolase	40	6.69, 47.4	86	2.5×10^{-9}
Dihydrolipoamide *S*-succinyltransferase	29	4.41, 49.3	76	2.5×10^{-8}
Pyruvate dehydrogenase	45	6.41, 39.2	65	3.2×10^{-7}
Aspartate aminotransferase	21	6.68, 46.5	82	6.3×10^{-9}
CK	32	5.52, 42.9	178	1.6×10^{-18}
Aconitase	14	5.43, 86.5	90	1.0×10^{-9}
γ-Enolase (NSE)	12	6.71, 47.6	145	3.2×10^{-15}
HSP90	21	4.97, 83.5	74	4.0×10^{-8}
VDAC-1	19	8.55, 32.5	73	5.0×10^{-8}

FIG. 3. *A*, *right*, 2D electrophoresis gel from supernatant of brain homogenate described in this study after immunoprecipitation by anti-VDAC-1 antibody. *Left*, 2D electrophoresis gel from brain of the mice described in this study. The *arrowhead* indicates that VDAC-1 disappears after immunoprecipitation, confirming its identity. *B*, *right*, 2D electrophoresis gel from supernatant of brain homogenate described in this study after immunoprecipitation by anti-HSP90 antibody. *Left*, 2D electrophoresis gel from brain of the mice described in this study. The *arrowhead* indicates that HSP90 disappears after immunoprecipitation, confirming its identity.
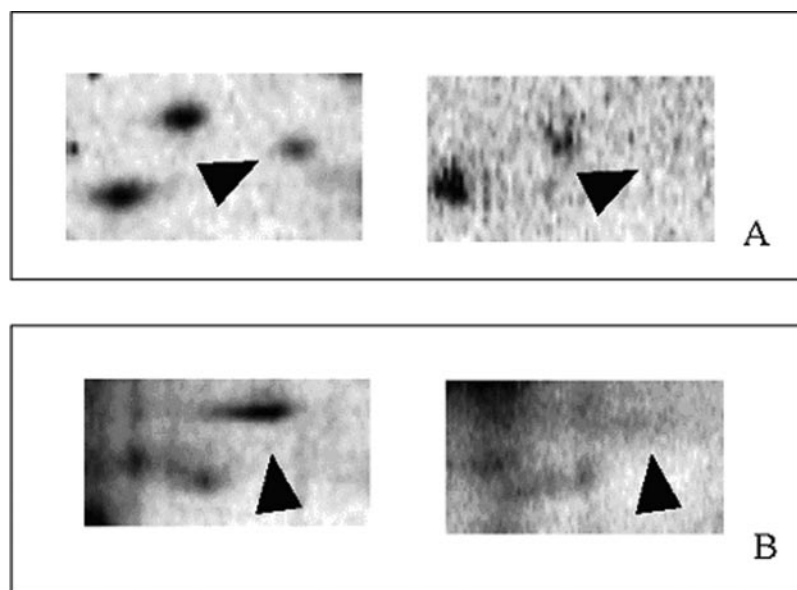
RESULTS

Protein Expression Levels—Two-dimensional electrophoresis offers an efficient tool to screen for abundant protein changes in different disease states as well as differences in metabolic pathways (30). The striatum proteome of R6/2 transgenic mice was investigated and compared with age-matched controls (4- and 10-week-old mice) using two-dimensional electrophoresis. Striatum was used for the present study because it is widely accepted that there is a selective pattern of neuronal degeneration in HD, and the neostriatum is the primary site of involvement (31). Our study entailed a four-way comparison, comprising four distinct groups of protein samples to be analyzed, because not only control mice (non-transgenic mice) are compared with R6/2 transgenic mice, but additionally, mice are compared with regard to their age. Thus, the final comparisons performed in the present study involved: 1) 4-week-old R6/2 mice *versus* 4-week-old CTR mice, 2) 10-week-old R6/2 mice *versus* 4-week-old R6/2 mice, 3) 10-week-old R6/2 mice *versus* 10-week-old CTR mice, and 4) 10-week-old CTR mice *versus* 4-week-old CTR mice. The latter group was studied to normalize differences in

protein expression and oxidation related exclusively to aging and not to the disease. Fig. 1 shows a typical 2D gel after SYPRO Ruby staining, and Fig. 2 shows a typical 2D Western blot for each group. The proteins identified by mass spectrometry and bioinformatics are listed in Table I. To validate the proteomic identification, we used anti-heat shock protein 90 (HSP90) and anti-VDAC-1 antibody to immunoprecipitate these two proteins from brain homogenate. Upon immunoprecipitation, the spots were absent in the 2D gels (Fig. 3). Thus, the identification of the HSP90 and VDAC-1 is validated by immunochemistry, indicating that identification of proteins by mass spectrometry is equivalent to those by immunochemistry.

The proteins that were expressed differentially in R6/2 mice are summarized in Table II. The expression levels of α-enolase were significantly increased in 4-week-old R6/2 mice compared with their age-matched controls and remain almost expressed at the same levels in 10-week-old transgenic mice. In addition, we observed an increase of dihydrolipoamide *S*-succinyltransferase and aspartate aminotransferase expression levels in 10-week-old R6/2 mice with respect to

TABLE II

Change of protein expression levels in 10-week-old R6/2 transgenic mice compared with 4-week-old transgenic mice and with non-transgenic mice (n = 6 for each group)

Values are expressed as percentage of control ± S.E. Yg HD *vs.* Yg CTR, 4-week-old HD transgenic mice *versus* young CTR mice; Old HD *vs.* Yg HD, 10-week-old HD transgenic mice *versus* 4-week-old HD transgenic mice; Old HD *vs.* old CTR, 10-week-old HD transgenic mice *versus* 10-week-old CTR mice.

Identified protein	Protein levels (percentage of control ± S.E.)	Yg HD *vs.* Yg CTR	Old HD *vs.* Yg HD	Old HD *vs.* old CTR	*p* value
α-Enolase	140 ± 8	√			<0.001
Dihydrolipoamide *S*-succinyltransferase	320 ± 28		√		<0.05
Pyruvate dehydrogenase	40 ± 5		√		<0.005
Aspartate aminotransferase	180 ± 9			√	<0.05

FIG. 4. **Activity of enolase in 10-week-old R6/2 mice as percent control of the age-matched non-transgenic control.** The activity of enolase is significantly decreased in the R6/2 mice. *Columns* represent mean ± S.E.*, *p* < 0.05; *n* = 5 for each group.
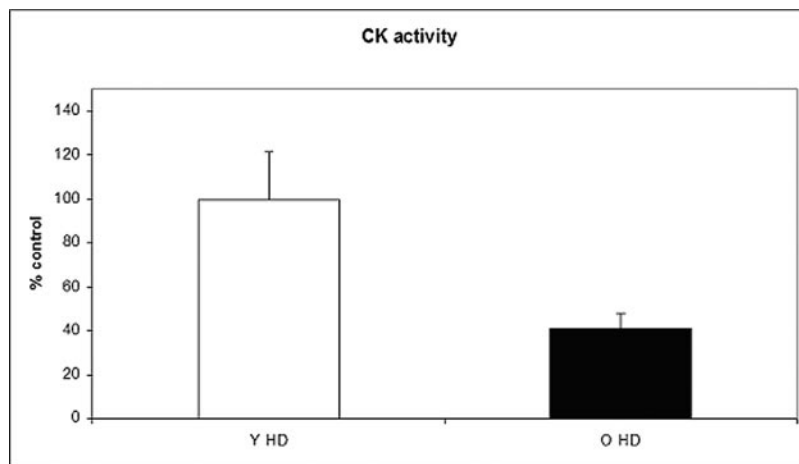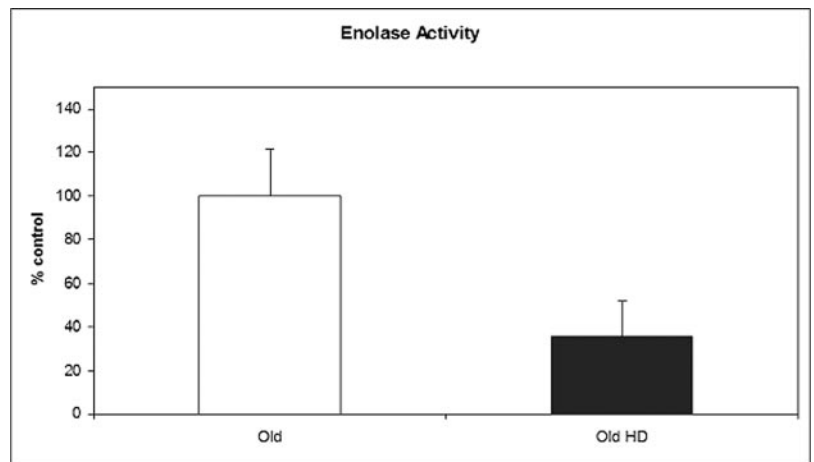

FIG. 5. **Activity of CK in 10-week-old R6/2 mice as percent control of the 4-week-old R6/2 mice.** The activity of CK is significantly decreased in the 10-week-old R6/2 mice. *Columns* represent mean ± S.E.*, *p* < 0.05; *n* = 5 for each group. *Y*, young; *O*, old.

4-week-old transgenic mice, whereas pyruvate dehydrogenase protein levels were found to be decreased in the same comparison groups.

Specific Protein Carbonyl Levels—The specific carbonyl levels were obtained by dividing the carbonyl level of a protein spot on the nitrocellulose membrane by the protein level of its corresponding protein spot on the gel. Such number gives the carbonyl level per unit of protein. We used a parallel approach to quantify the protein levels by SYPRO Ruby staining and the extent of DNP-bound proteins by immunohistochemistry (Fig. 2). We found that in comparison with age-matched control mice, R6/2 mice have six proteins that are significantly more oxidized. These proteins are α-enolase, γ-enolase (neuron-specific enolase), VDAC-1, creatine kinase (CK), aconitase, and HSP90. Moreover the activity of enolase of R6/2 mice was decreased when compared with the age-matched control (Fig. 4). Interestingly we could demonstrate that the oxidation of CK and aconitase occurred over the course of the disease

Increased protein carbonyl levels in 10-week-old R6/2 mice compared with 4-week-old transgenic mice and with their age-matched controls (n = 6 for each group)

Values are expressed as -fold increase. Old HD *vs*. Yg HD, 10-week-old HD transgenic mice *versus* 4-week-old HD transgenic mice; Old HD *vs*. old CTR, 10-week-old HD transgenic mice *versus* 10-week-old CTR mice.

Identified protein	Mean -fold increase in protein carbonyl levels	Old HD *vs*. Yg HD	Old HD *vs*. old CTR	*p* value
α-Enolase	3.7 ± 0.79		√	<0.005
γ-Enolase (NSE)	23.9 ± 17.4		√	<0.05
Aconitase	7.9 ± 2.25	√		<0.001
CK	3.1 ± 0.94	√		<0.005
VDAC-1	2.4 ± 0.38		√	<0.001
HSP90	133 ± 7.95		√	<0.005

(10-week-old *versus* 4-week-old R6/2 transgenic mice) as a result of the neurodegenerative processes associated with "Huntington" pathology. The decreased activity in 10-week-old R6/2 transgenic mice when compared with that of 4-week-old R6/2 transgenic mice (Fig. 5) confirmed the notion that oxidative modification of a enzyme leads to its dysfunction. The summary of specific carbonyl levels of the six identified proteins is shown in Table III.

We used the Interaction Explorer Software PathwayAssist (Stratagene) to show the functional interactions between the proteins of interest by searching a database built by the MedScan text-mining algorithms to all PubMed abstracts. These interactions between the proteins of interest, that we have identified in our current study, were visualized in an interaction network or interactome (Fig. 6). This interaction network indicated that the identified proteins are involved in metabolism and mitochondrial function.

DISCUSSION

The development of transgenic mouse models of neurodegenerative diseases provides a major advance for studying disease pathogenesis and for developing therapeutic agents. We used proteomics to investigate the expression of proteins and their oxidative stress in the striata from R6/2 transgenic mice, the most widely used model of Huntington disease. We demonstrated that the protein expression levels of α-enolase, dihydrolipoamide *S*-succinyltransferase, pyruvate dehydrogenase, and aspartate aminotransferase were significantly changed in 10-week-old transgenic mice compared either with their age-matched control or with 4-week-old transgenic mice. In addition, our analysis has shown that the specific protein carbonyl levels of α- and γ-enolase isoforms, aconitase, CK, HSP90, and VDAC-1 were significantly increased in the same sets of comparison.

Oxidative damage has been identified as a feature of neurodegenerative diseases including AD, Parkinson disease, and Friedrich ataxia (32). Polyglutamine-expanded proteins induce DNA damage *in vitro* (33), and there is evidence of increased oxidative damage in postmortem brain tissue of patients with HD (1). In R6/2 transgenic mice increased levels of 3-nitrotyrosine, increased lipid peroxidation, and age-dependent progressive increase in 8-hydroxy-2-deoxyguanosine, a marker of oxidative damage to DNA, have been reported (6, 34, 35).

The current study shows that the protein expression levels of α-enolase are increased as early as primary signs of the pathology are observed in R6/2 transgenic (4-week-old) mice. Consistent with this result, learning impairment, brain weight reduction, and neuronal intranuclear inclusions can be detected at 4 weeks of age (23, 36). At this early stage of the disease process, most of the molecular changes occur at mRNA levels (37, 38). Interestingly investigating the disease on the protein level could offer increased insight into the development of neurodegeneration in this and other diseases.

α-Enolase is a subunit of enolase, the enzyme that catalyzes the dehydration of 2-phospho-D-glycerate to form phosphoenolpyruvate. In mammals, the active form of the enzyme is a dimer (homo- and heterodimer) consisting of three different subunits: α, β, and γ. In human brain, enolase exists in three molecular forms: non-neuronal enolase (α, α'-enolase), neuron-specific enolase (NSE; γ, γ'-enolase, also known as 14-3-2 protein and neuron specific protein), and the short lived heterodimer α, γ'-enolase. This enzyme has been studied extensively in AD brain, and recently our proteomic investigation has identified α-enolase as specifically oxidized in AD brain (39) and in the G93A-SOD1 transgenic mice model of fALS (40). Here we found not only an increase of α-enolase protein levels but also a parallel increment of its specific carbonyl levels. Thus, oxidative modification can lead to structural alteration and activity decline of α-enolase as we observed in the current study, suggesting that the reduced enzyme activity is compensated by its increased expression.

α-Enolase is present during embryonic development and switches to γ or β concurrently with terminal differentiation of the muscle or neuron (41). Because γ isoforms are predominantly found in the brain, they are called NSE (42). NSE has been used as a neuronal marker for structural damage and as a marker for neuronal metabolic properties (43). It has also been reported that the expression of NSE coincides with the onset of synaptic connections (44). Therefore,
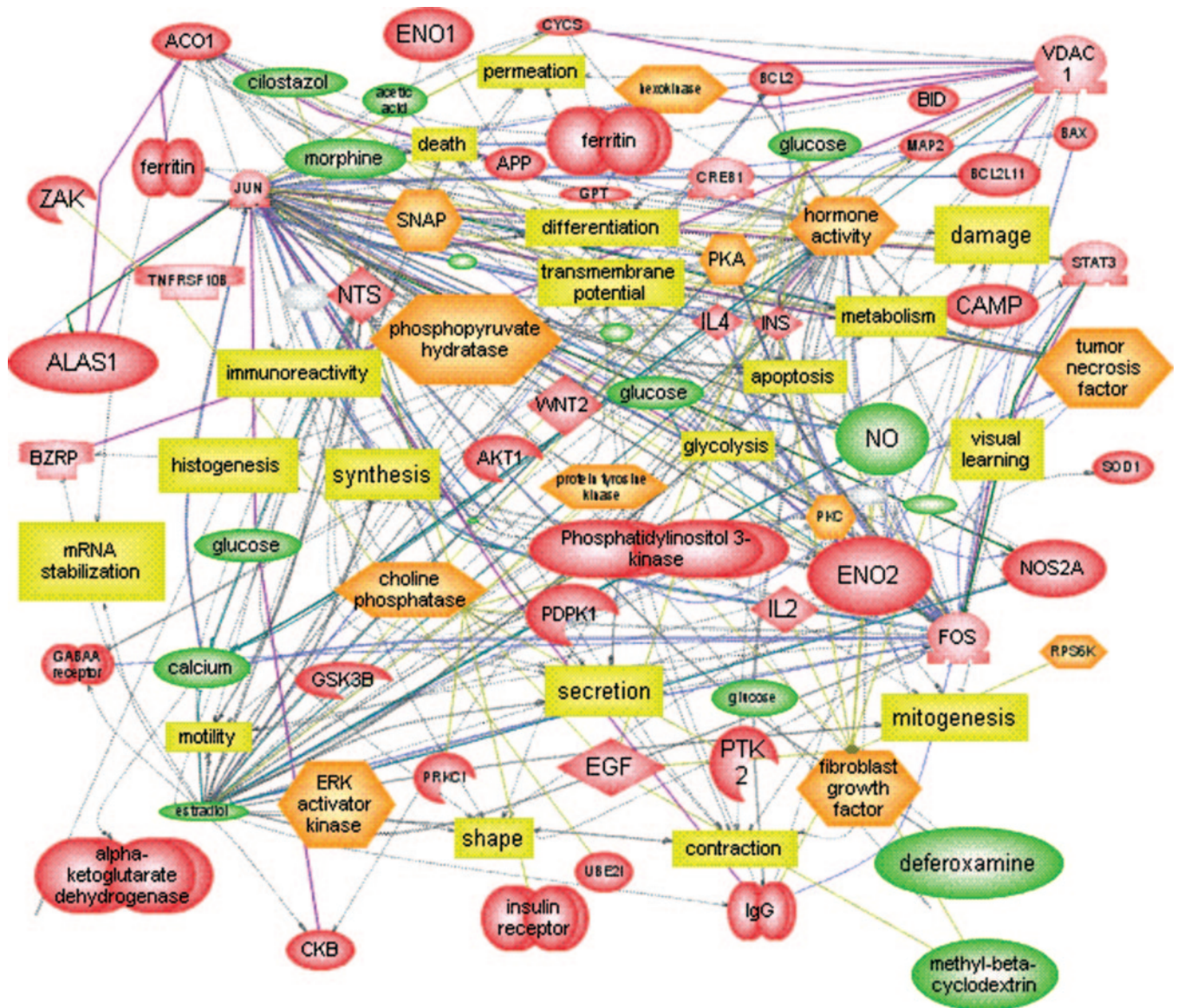
FIG. 6. **Schematic diagram of a functional interactome of all the proteins identified to be significantly oxidatively modified.** This diagram was generated by the Interaction Explorer Pathway Module (Stratagene), indicating that all the proteins directly or indirectly are associated with cellular processes shown.

enolase is not only involved in metabolism but also in cell differentiation and normal growth in the brains. In the present study, we demonstrated increased carbonyl levels of both α- and γ-enolase isoforms, and the activity of enolase is correspondingly decreased, suggesting that oxidative modifications could lead to a reduced metabolism and to abnormal neuronal growth of R6/2 mouse brain and potentially HD brain as well.

The analysis of the R6/2 protein expression profile has also shown an increase of protein expression levels of dihydrolipoamide *S*-succinyltransferase and reduced levels of pyruvate dehydrogenase over the course of the disease (10-week-old *versus* 4-week-old R6/2 transgenic mice). Furthermore the induction of aspartate aminotransferase expression levels be-

came apparent in 10-week-old transgenic mice compared with their age-matched controls.

Dihydrolipoamide *S*-succinyltransferase (E2) is the structural and catalytic core of the 2-oxo acid dehydrogenase multienzyme complexes that catalyze CoA- and NAD$^+$-linked and lipoic acid-mediated decarboxylation of 2-oxo acids. Namely the pyruvate dehydrogenase complex and α-ketoglutarate dehydrogenase complex are part of this family of complexes, consisting of three different subunits, 2-oxoglutarate dehydrogenase (E1), E2, and lipoamide dehydrogenase (E3). The increase of dihydrolipoamide *S*-succinyltransferase and the parallel reduction of pyruvate dehydrogenase (PDHC) expression levels may lead to a discrepancy. Many authors reported that the activity of PDHC was reduced in affected

areas of brains (basal ganglia and hippocampus) from patients with Huntington disease (45, 46). The induction of one of the subunits of the multienzyme complex may be regarded as an attempt to compensate for the whole activity reduction of PDHC even if the regulation of the enzyme requires its phosphorylation.

The impairment of energy metabolism has been shown to selectively contribute to neurodegenerative processes in HD. Mitochondrial defects may result from oxidative damage to cellular elements or alternatively may induce oxidative stress via increased free radical production. Consequently biochemical studies in HD postmortem tissue have revealed alterations in the activity of several key components of oxidative phosphorylation and the tricarboxylic acid cycle in brain regions targeted in HD. Activities of complexes II, III, and IV of the electron transport chain are markedly and selectively reduced in caudate and putamen of advanced HD patients (8). The most profound defect detected in HD to date is the dramatic reduction in activity of the tricarboxylic acid cycle enzyme aconitase in affected brain regions and muscle. Interestingly in this study we found increased carbonyl levels of aconitase. This enzyme is an iron-sulfur protein that catalyzes the stereospecific isomerization of citrate to isocitrate via *cis*-aconitate, a reaction essential to normal metabolic function. The particular susceptibility of mitochondrial aconitase to oxidative damage may be related to the iron-sulfur cluster [4Fe-4S] in its active site (47). Studies *in vitro* established that aconitase is particularly sensitive to reaction with superoxide (48, 49), which causes release of one iron atom from the cluster (50). Inactivation of aconitase may block normal electron flow to oxygen, leading to an accumulation of reduced metabolites such as NADH. Therefore, oxidative inactivation of aconitase can initiate a cascade with the potential to cause a dramatic increase in the cellular burden of oxidative damage. Based on these notions, the induction of protein expression levels of aspartate aminotransferase may be regarded as an attempt to restore the tricarboxylic acid cycle. This enzyme catalyzes the conversion of aspartate to its corresponding oxo acid α-ketoglutarate, which is produced downstream to the aconitase reaction. Thus, the inactivation of aconitase blocks the subsequent production of α-ketoglutarate, which may be partially restored through the transamination of aspartate operated by aspartate aminotransferase.

Oxidatively modified proteins are generally dysfunctional, losing catalytic or structural integrity (29, 51, 52). Oxidative damage to proteins is of importance in explaining metabolic dysfunctions associated to oxidative stress-mediated diseases. It is conceivable that increased oxidative modification of brain proteins may disturb neuronal functions by decreasing activities of key metabolic enzymes and affecting cellular signaling systems (53, 54).

Bioenergetic defects are a profound feature of Huntington disease; thus our finding of increased carbonyl levels and decreased activity of CK further determines which crucial enzymes are finely involved in energetic impairments in this disorder. The CK system, consisting of a cytosolic and a mitochondrial isoform (MtCK) together with their substrates creatine and phosphocreatine, is the most important immediate energy buffering and transport system of the cell (55) especially in muscle and neuronal tissue (56). Creatine is phosphorylated to phosphocreatine in the intermembrane space of mitochondria where mitochondrial CK is located and is then transported into the cytosol (57). There the energy pool can be regenerated by transphosphorylation of phosphocreatine to ATP, which is catalyzed by cytosolic CK located in close vicinity of cellular ATPases. CKs are prime targets of oxidative damage (58–60), leading to inactivation of both isoforms. Additionally reactive oxygen species lead to dimerization of MtCK (61). Inactivation of CK and dimerization of MtCK are both expected to contribute to a deterioration of the cellular energy state (62). Consistent with others, we showed that oxidative modifications of CK decrease its activity during aging and neurodegenerative diseases (20, 60, 63). Recent reports have demonstrated that creatine therapy provides neuroprotection and delays motor symptoms in transgenic animal model of HD (64, 65), thus suggesting enhancement of cerebral energy metabolism as a protective mechanism against neurodegeneration.

Our current study indicates loss of activity, caused by oxidative modification, of the enzymes involved in glucose metabolism, such as α- and γ-enolase, pyruvate dehydrogenase, and aconitase, and of CK might lead to a reduced ATP production. In addition, loss of energy production by mitochondria can result in diminution of ATP synthesis and thus disruption of cellular functions that depend on ATP, including metabolite levels and ionic gradients. The latter can have a serious consequence for Ca^{2+} entry to neurons and maintenance of metabolic potential.

Recently many authors have focused their attention to determine a direct link between the huntingtin mutation and mitochondrial defects. Evidence is gradually emerging that the mutant protein may directly interact with neuronal mitochondria, consequently leading to their degeneration (66). The degeneration is typified by mitochondrial swelling, disruption of the cristae and mitochondrial membranes, and eventual condensation and lysosomal engulfment.

Functional changes in mitochondria caused by mutant huntingtin also have been shown recently by the demonstration that polyglutamines can influence mitochondrial calcium handling. Panov *et al.* (67, 68) indicated that mitochondrial Ca^{2+} homeostasis is compromised in HD and suggested that the permeability transition pore (PTP) opening is central to this phenomenon. It is still uncertain how the calcium retention capacity decreases. Our finding of increased protein carbonyl levels of VADC-1 offers a reasonable explanation for calcium overload and PTP-induced mitochondrial dysfunction observed in HD mouse models and human brain. The transition pore is formed from a complex of the VDAC, the

adenine dinucleotide translocase, and cyclophilin-D at contact sites between the mitochondrial inner and outer membranes. Here we propose that oxidative modification of VADC-1 might change its functional properties thus contributing to disruption of PTP permeability. This would lead to a lower Ca^{2+} threshold for depolarization, to collapse of $\Delta\psi_m$, and ultimately to alteration of mitochondrial permeability transition. Induction of mitochondrial permeability transition results in mitochondrial swelling with release of cytochrome *c* and subsequent activation of the apoptotic cascade (69). Our hypotheses is consistent with the finding reported by Panov *et al.* (70) that mutant huntingtin is associated with the outer mitochondrial membrane and thus may directly impair mitochondrial function. These authors also demonstrated that HD mitochondria have a lower membrane potential and depolarize at lower calcium loads than do mitochondria from controls (67). Our results are consistent with the notion that the "toxic gain of function" of mutant huntingtin promotes structural changes of functional proteins by rendering them more susceptible to oxidative stress or by inducing oxidative conditions in the sites of huntingtin accumulation.

Evidence has been presented that the formation of neuronal inclusions with aggregated huntingtin protein is associated with the progressive neuropathology in HD (36). Accumulation of misfolded proteins is one of the major causes of neurodegenerative disorders like AD, ALS, and HD (71). Neuronal cells recognize the aggregated huntingtin protein as abnormally folded and, by recruiting molecular chaperones (HSPs) and proteosomal components, try to disaggregate and/or degrade the mutant protein. Conversely the toxicity of mutant huntingtin may reduce the availability of HSPs, thereby disrupting their normal chaperone and anti-apoptotic functions and reducing their cytoprotective effects (72). Consistent with this view, we found increased carbonyl levels of HSP90. Here we propose that diminished degradation of mutant aggregated huntingtin is possibly related to inactivation of HSP90, which once oxidatively modified is not able to facilitate misfolded protein degradation by the proteasome. Recent studies reported that the activation of the heat shock response inhibits huntingtin aggregation in a cell culture model of HD (73). Moreover Kieran *et al.* (74) have shown that the treatment with a coinducer of HSPs significantly delays disease progression in a transgenic mouse model of ALS. Pharmacological activation of the HSP response may therefore be a successful therapeutic approach for treating neurodegenerative disorders such as HD, ALS, and AD.

As indicated above, multiple lines of evidence indicate that oxidative stress and energetic defects may play roles in the etiology of selective neuronal death in HD. Using the Interaction Explorer Software PathwayAssist (Stratagene) to analyze our current results, proteins identified in this study are involved in metabolism and mitochondrial function. Therefore,

the results presented in the current study have provided a direct link between oxidative damage and bioenergetic impairment. Mitochondrial energy metabolism dysfunction may result from excessive oxidative damage to neuronal proteins as a consequence of increased free radical and oxidant generation. The slow, progressive nature of neuronal injury in chronic neurodegenerative disorders may be explained by cycling of free radicals and mitochondrial dysfunction. Thus, the identification of target proteins that are oxidatively modified may provide a vital insight into the etiologic role of oxidative damage in mechanisms of neuronal death in HD and other neurodegenerative disorders. Loss of activity of these proteins by oxidative modification or by altered expression may contribute to abnormal metabolism and neurochemical changes ultimately leading to neuronal death. Our current study forms a framework for subsequent experiments and provides potential new targets for neuroprotective therapeutic intervention in HD.

j To whom correspondence should be addressed: Dept. of Chemistry, Center of Membrane Sciences, and Sanders-Brown Center on Aging, University of Kentucky, Lexington, KY 40506-0055. Tel.: 859-257-3184; Fax: 859-257-5876; E-mail: dabcns@uky.edu.

REFERENCES

1. Browne, S. E., Ferrante, R. J., and Beal, M. F. (1999) Oxidative stress in Huntington's disease. *Brain Pathol.* **9,** 147–163
2. Andrew, S. E., Goldberg, Y. P., Kremer, B., Telenius, H., Theilmann, J., Adam, S., Starr, E., Squitieri, F., Lin, B., Kalchman, M. A., Graham, R. K., and Hayden, M. R. (1993) The relationship between trinucleotide (CAG) repeat length and clinical features of Huntington's disease. *Nat. Genet.* **4,** 398–403
3. Snell, R. G., MacMillan, J. C., Cheadle, J. P., Fenton, I., Lazarou, L. P., Davies, P., MacDonald, M. E., Gusella, J. F., Harper, P. S., and Shaw, D. J. (1993) Relationship between trinucleotide repeat expansion and phenotypic variation in Huntington's disease. *Nat. Genet.* **4,** 393–397
4. Beal, M. F., and Ferrante, R. J. (2004) Experimental therapeutics in transgenic mouse models of Huntington's disease. *Nat. Rev. Neurosci.* **5,** 373–384
5. Diaz-Hernandez, M., Hernandez, F., Martin-Aparicio, E., Gomez-Ramos, P., Moran, M. A., Castano, J. G., Ferrer, I., Avila, J., and Lucas, J. J. (2003) Neuronal induction of the immunoproteasome in Huntington's disease. *J. Neurosci.* **23,** 11653–11661
6. Bogdanov, M. B., Andreassen, O. A., Dedeoglu, A., Ferrante, R. J., and Beal, M. F. (2001) Increased oxidative damage to DNA in a transgenic mouse model of Huntington's disease. *J. Neurochem.* **79,** 1246–1249
7. Petersen, A., Hansson, O., Puschban, Z., Sapp, E., Romero, N., Castilho, R. F., Sulzer, D., Rice, M., DiFiglia, M., Przedborski, S., and Brundin, P. (2001) Mice transgenic for exon 1 of the Huntington's disease gene display reduced striatal sensitivity to neurotoxicity induced by dopamine and 6-hydroxydopamine. *Eur. J. Neurosci.* **14,** 1425–1435
8. Browne, S. E., Bowling, A. C., MacGarvey, U., Baik, M. J., Berger, S. C., Muqit, M. M., Bird, E. D., and Beal, M. F. (1997) Oxidative damage and metabolic dysfunction in Huntington's disease: selective vulnerability of the basal ganglia. *Ann. Neurol.* **41,** 646–653

9. Polidori, M. C., Mecocci, P., Browne, S. E., Senin, U., and Beal, M. F. (1999) Oxidative damage to mitochondrial DNA in Huntington's disease parietal cortex. *Neurosci. Lett.* **272,** 53–56

10. Tabrizi, S. J., Cleeter, M. W., Xuereb, J., Taanman, J. W., Cooper, J. M., and Schapira, A. H. (1999) Biochemical abnormalities and excitotoxicity in Huntington's disease brain. *Ann. Neurol.* **45,** 25–32

11. Brouillet, E., Hantraye, P., Ferrante, R. J., Dolan, R., Leroy-Willig, A., Kowall, N. W., and Beal, M. F. (1995) Chronic mitochondrial energy impairment produces selective striatal degeneration and abnormal choreiform movements in primates. *Proc. Natl. Acad. Sci. U. S. A.* **92,** 7105–7109

12. Browne, S. E., and Beal, M. F. (1994) Oxidative damage and mitochondrial dysfunction in neurodegenerative diseases. *Biochem. Soc. Trans.* **22,** 1002–1006

13. Fagni, L., Lafon-Cazal, M., Rondouin, G., Manzoni, O., Lerner-Natoli, M., and Bockaert, J. (1994) The role of free radicals in NMDA-dependent neurotoxicity. *Prog. Brain Res.* **103,** 381–390

14. Beal, M. F. (2002) Oxidatively modified proteins in aging and disease. *Free Radic. Biol. Med.* **32,** 797–803

15. Beckman, K. B., and Ames, B. N. (1997) Oxidative decay of DNA. *J. Biol. Chem.* **272,** 19633–19636

16. Butterfield, D. A., Howard, B. J., and LaFontaine, M. A. (2001) Brain oxidative stress in animal models of accelerated aging and the age-related neurodegenerative disorders, Alzheimer's disease and Huntington's disease. *Curr. Med. Chem.* **8,** 815–828

17. Stadtman, E. R., and Berlett, B. S. (1997) Reactive oxygen-mediated protein oxidation in aging and disease. *Chem. Res. Toxicol.* **10,** 485–494

18. Korolainen, M. A., Goldsteins, G., Alafuzoff, I., Koistinaho, J., and Pirttila, T. (2002) Proteomic analysis of protein oxidation in Alzheimer's disease brain. *Electrophoresis* **23,** 3428–3433

19. Butterfield, D. A., and Lauderback, C. M. (2002) Lipid peroxidation and protein oxidation in Alzheimer's disease brain: potential causes and consequences involving amyloid beta-peptide-associated free radical oxidative stress. *Free Radic. Biol. Med.* **32,** 1050–1060

20. Poon, H. F., Castegna, A., Farr, S. A., Thongboonkerd, V., Lynn, B. C., Banks, W. A., Morley, J. E., Klein, J. B., and Butterfield, D. A. (2004) Quantitative proteomics analysis of specific protein expression and oxidative modification in aged senescence-accelerated-prone 8 mice brain. *Neuroscience.* **126,** 915–926

21. Mangiarini, L., Sathasivam, K., Seller, M., Cozens, B., Harper, A., Hetherington, C., Lawton, M., Trottier, Y., Lehrach, H., Davies, S. W., and Bates, G. P. (1996) Exon 1 of the HD gene with an expanded CAG repeat is sufficient to cause a progressive neurological phenotype in transgenic mice. *Cell* **87,** 493–506

22. Carter, R. J., Lione, L. A., Humby, T., Mangiarini, L., Mahal, A., Bates, G. P., Dunnett, S. B., and Morton, A. J. (1999) Characterization of progressive motor deficits in mice transgenic for the human Huntington's disease mutation. *J. Neurosci.* **19,** 3248–3257

23. Lione, L. A., Carter, R. J., Hunt, M. J., Bates, G. P., Morton, A. J., and Dunnett, S. B. (1999) Selective discrimination learning impairments in mice expressing the human Huntington's disease mutation. *J. Neurosci.* **19,** 10428–10437

24. Levine, R. L., Williams, J. A., Stadtman, E. R., and Shacter, E. (1994) Carbonyl assays for determination of oxidatively modified proteins. *Methods Enzymol.* **233,** 346–357

25. Thongboonkerd, V., McLeish, K. R., Arthur, J. M., and Klein, J. B. (2002) Proteomic analysis of normal human urinary proteins isolated by acetone precipitation or ultracentrifugation. *Kidney Int.* **62,** 1461–1469

26. Butterfield, D. A., Boyd-Kimball, D., and Castegna, A. (2003) Proteomics in Alzheimer's disease: insights into potential mechanisms of neurodegeneration. *J Neurochem.* **86,** 1313–1327

27. Lauderback, C. M., Hackett, J. M., Huang, F. F., Keller, J. N., Szweda, L. I., Markesbery, W. R., and Butterfield, D. A. (2001) The glial glutamate transporter, GLT-1, is oxidatively modified by 4-hydroxy-2-nonenal in the Alzheimer's disease brain: the role of Aβ1–42. *J Neurochem.* **78,** 413–416

28. Wagner, S., Breiteneder, H., Simon-Nobbe, B., Susani, M., Krebitz, M., Niggemann, B., Brehler, R., Scheiner, O., and Hoffmann-Sommergruber, K. (2000) Hev b 9, an enolase and a new cross-reactive allergen from hevea latex and molds. Purification, characterization, cloning and expression. *Eur. J. Biochem.* **267,** 7006–7014

29. Fai Poon, H., Frasier, M., Shreve, N., Calabrese, V., Wolozin, B., and Butterfield, D. A. (2005) Mitochondrial associated metabolic proteins are selectively oxidized in A30P α-synuclein transgenic mice-a model of familial Parkinson's disease. *Neurobiol. Dis.* **18,** 492–498

30. Butterfield, D. A., and Castegna, A. (2003) Proteomics for the identification of specifically oxidized proteins in brain: technology and application to the study of neurodegenerative disorders. *Amino Acids* **25,** 419–425

31. Vonsattel, J. P., and DiFiglia, M. (1998) Huntington disease. *J. Neuropathol. Exp. Neurol.* **57,** 369–384

32. Butterfield, D. A., and Kanski, J. (2001) Brain protein oxidation in age-related neurodegenerative disorders that are associated with aggregated proteins. *Mech. Ageing Dev.* **122,** 945–962

33. Giuliano, P., De Cristofaro, T., Affaitati, A., Pizzulo, G. M., Feliciello, A., Criscuolo, C., De Michele, G., Filla, A., Avvedimento, E. V., and Varrone, S. (2003) DNA damage induced by polyglutamine-expanded proteins. *Hum. Mol. Genet.* **12,** 2301–2309

34. Tabrizi, S. J., Orth, M., Wilkinson, J. M., Taanman, J. W., Warner, T. T., Cooper, J. M., and Schapira, A. H. (2000) Expression of mutant α-synuclein causes increased susceptibility to dopamine toxicity. *Hum. Mol. Genet.* **9,** 2683–2689

35. Perez-Severiano, F., Rios, C., and Segovia, J. (2000) Striatal oxidative damage parallels the expression of a neurological phenotype in mice transgenic for the mutation of Huntington's disease. *Brain Res.* **862,** 234–237

36. Davies, S. W., Turmaine, M., Cozens, B. A., DiFiglia, M., Sharp, A. H., Ross, C. A., Scherzinger, E., Wanker, E. E., Mangiarini, L., and Bates, G. P. (1997) Formation of neuronal intranuclear inclusions underlies the neurological dysfunction in mice transgenic for the HD mutation. *Cell* 90, 537–548

37. Augood, S. J., Faull, R. L., Love, D. R., and Emson, P. C. (1996) Reduction in enkephalin and substance P messenger RNA in the striatum of early grade Huntington's disease: a detailed cellular in situ hybridization study. *Neuroscience* **72,** 1023–1036

38. Luthi-Carter, R., Strand, A., Peters, N. L., Solano, S. M., Hollingsworth, Z. R., Menon, A. S., Frey, A. S., Spektor, B. S., Penney, E. B., Schilling, G., Ross, C. A., Borchelt, D. R., Tapscott, S. J., Young, A. B., Cha, J. H., and Olson, J. M. (2000) Decreased expression of striatal signaling genes in a mouse model of Huntington's disease. *Hum. Mol. Genet.* **9,** 1259–1271

39. Castegna, A., Aksenov, M., Thongboonkerd, V., Klein, J. B., Pierce, W. M., Booze, R., Markesbery, W. R., and Butterfield, D. A. (2002) Proteomic identification of oxidatively modified proteins in Alzheimer's disease brain. Part II: dihydropyrimidinase-related protein 2, α-enolase and heat shock cognate 71. *J. Neurochem.* **82,** 1524–1532

40. Perluigi, M., Fai Poon, H., Hensley, K., Pierce, W. M., Klein, J. B., Calabrese, V., De Marco, C., and Butterfield, D. A. (2005) Proteomic analysis of 4-hydroxy-2-nonenal-modified proteins in G93A-SOD1 transgenic mice—a model of familial amyotrophic lateral sclerosis. *Free Radic. Biol. Med.* **38,** 960–968

41. Giallongo, A., Oliva, D., Cali, L., Barba, G., Barbieri, G., and Feo, S. (1990) Structure of the human gene for α-enolase. *Eur. J. Biochem.* **190,** 567–573

42. Keller, A., Berod, A., Dussaillant, M., Lamande, N., Gros, F., and Lucas, M. (1994) Coexpression of α and γ enolase genes in neurons of adult rat brain. *J. Neurosci. Res.* **38,** 493–504

43. el-Mallakh, R. S., Egan, M., and Wyatt, R. J. (1992) Creatine kinase and enolase: intracellular enzymes serving as markers of central nervous system damage in neuropsychiatric disorders. *Psychiatry* **55,** 392–402

44. Maxwell, G. D., Whitehead, M. C., Connolly, S. M., and Marangos, P. J. (1982) Development of neuron-specific enolase immunoreactivity in avian nervous tissue *in vivo* and *in vitro*. *Brain Res.* **255,** 401–418

45. Sorbi, S., Bird, E. D., and Blass, J. P. (1983) Decreased pyruvate dehydrogenase complex activity in Huntington and Alzheimer brain. *Ann. Neurol.* **13,** 72–78

46. Butterworth, J., Yates, C. M., and Reynolds, G. P. (1985) Distribution of phosphate-activated glutaminase, succinic dehydrogenase, pyruvate dehydrogenase and gamma-glutamyl transpeptidase in post-mortem brain from Huntington's disease and agonal cases. *J. Neurol. Sci.* **67,** 161–171

47. Kent, T. A., Dreyer, J. L., Kennedy, M. C., Huynh, B. H., Emptage, M. H.,

Beinert, H., and Munck, E. (1982) Mossbauer studies of beef heart aconitase: evidence for facile interconversions of iron-sulfur clusters. *Proc. Natl. Acad. Sci. U. S. A.* **79,** 1096–1100

48. Gardner, P. R., Nguyen, D. D., and White, C. W. (1994) Aconitase is a sensitive and critical target of oxygen poisoning in cultured mammalian cells and in rat lungs. *Proc. Natl. Acad. Sci. U. S. A.* **91,** 12248–12252

49. Verniquet, F., Gaillard, J., Neuburger, M., and Douce, R. (1991) Rapid inactivation of plant aconitase by hydrogen peroxide. *Biochem. J.* **276,** 643–648

50. Flint, D. H., Tuminello, J. F., and Emptage, M. H. (1993) The inactivation of Fe-S cluster containing hydrolases by superoxide. *J. Biol. Chem.* **268,** 22369–22376

51. Levine, R. L., and Stadtman, E. R. (1996) in *Handbook of the Biology of Aging* (Schneider, E. L., and Rowe, J. W., eds) 4th Ed., pp. 184–197, Academic Press, San Diego, CA

52. Subramaniam, R., Roediger, F., Jordan, B., Mattson, M. P., Keller, J. N., Waeg, G., and Butterfield, D. A. (1997) The lipid peroxidation product, 4-hydroxy-2-trans-nonenal, alters the conformation of cortical synaptosomal membrane proteins. *J. Neurochem.* **69,** 1161–1169

53. Smith, C. D., Carney, J. M., Tatsumo, T., Stadtman, E. R., Floyd, R. A., and Markesbery, W. R. (1992) Protein oxidation in aging brain. *Ann. N. Y. Acad. Sci.* **663,** 110–119

54. Malorni, W., Rainaldi, G., Rivabene, R., Santini, M. T., Peterson, S. W., Testa, U., and Donelli, G. (1994) Cytoskeletal oxidative changes lead to alterations of specific cell surface receptors. *Eur. J. Histochem.* **38,** Suppl. 1, 91–100

55. Wallimann, T., Dolder, M., Schlattner, U., Eder, M., Hornemann, T., O'Gorman, E., Ruck, A., and Brdiczka, D. (1998) Some new aspects of creatine kinase (CK): compartmentation, structure, function and regulation for cellular and mitochondrial bioenergetics and physiology. *Biofactors* **8,** 229–234

56. Wallimann, T., and Hemmer, W. (1994) Creatine kinase in non-muscle tissues and cells. *Mol. Cell. Biochem.* **133–134,** 193–220

57. Schlattner, U., Forstner, M., Eder, M., Stachowiak, O., Fritz-Wolf, K., and Wallimann, T. (1998) Functional aspects of the X-ray structure of mitochondrial creatine kinase: a molecular physiology approach. *Mol. Cell. Biochem.* **184,** 125–140

58. Dolder, M., Wendt, S., and Wallimann, T. (2001) Mitochondrial creatine kinase in contact sites: interaction with porin and adenine nucleotide translocase, role in permeability transition and sensitivity to oxidative damage. *Biol. Signals Recept.* **10,** 93–111

59. Konorev, E. A., Hogg, N., and Kalyanaraman, B. (1998) Rapid and irreversible inhibition of creatine kinase by peroxynitrite. *FEBS Lett.* **427,** 171–174

60. Castegna, A., Aksenov, M., Aksenova, M., Thongboonkerd, V., Klein, J. B., Pierce, W. M., Booze, R., Markesbery, W. R., and Butterfield, D. A. (2002) Proteomic identification of oxidatively modified proteins in Alzheimer's disease brain. Part I: creatine kinase BB, glutamine synthase, and ubiquitin carboxy-terminal hydrolase L-1. *Free Radic. Biol. Med.* **33,** 562–571

61. Soboll, S., Brdiczka, D., Jahnke, D., Schmidt, A., Schlattner, U., Wendt, S., Wyss, M., and Wallimann, T. (1999) Octamer-dimer transitions of mitochondrial creatine kinase in heart disease. *J. Mol. Cell. Cardiol.* **31,** 857–866

62. Stachowiak, O., Schlattner, U., Dolder, M., and Wallimann, T. (1998) Oligomeric state and membrane binding behaviour of creatine kinase isoenzymes: implications for cellular function and mitochondrial structure. *Mol. Cell. Biochem.* **184,** 141–151

63. Aksenov, M., Aksenova, M., Butterfield, D. A., and Markesbery, W. R. (2000) Oxidative modification of creatine kinase BB in Alzheimer's disease brain. *J. Neurochem.* **74,** 2520–2527

64. Dedeoglu, A., Kubilus, J. K., Yang, L., Ferrante, K. L., Hersch, S. M., Beal, M. F., and Ferrante, R. J. (2003) Creatine therapy provides neuroprotection after onset of clinical symptoms in Huntington's disease transgenic mice. *J. Neurochem.* **85,** 1359–1367

65. Andreassen, O. A., Dedeoglu, A., Ferrante, R. J., Jenkins, B. G., Ferrante, K. L., Thomas, M., Friedlich, A., Browne, S. E., Schilling, G., Borchelt, D. R., Hersch, S. M., Ross, C. A., and Beal, M. F. (2001) Creatine increase survival and delays motor symptoms in a transgenic animal model of Huntington's disease. *Neurobiol. Dis.* **8,** 479–491

66. Yu, Z. X., Li, S. H., Evans, J., Pillarisetti, A., Li, H., and Li, X. J. (2003) Mutant huntingtin causes context-dependent neurodegeneration in mice with Huntington's disease. *J. Neurosci.* **23,** 2193–2202

67. Panov, A. V., Gutekunst, C. A., Leavitt, B. R., Hayden, M. R., Burke, J. R., Strittmatter, W. J., and Greenamyre, J. T. (2002) Early mitochondrial calcium defects in Huntington's disease are a direct effect of polyglutamines. *Nat. Neurosci.* **5,** 731–736

68. Panov, A. V., Burke, J. R., Strittmatter, W. J., and Greenamyre, J. T. (2003) In vitro effects of polyglutamine tracts on Ca^{2+}-dependent depolarization of rat and human mitochondria: relevance to Huntington's disease. *Arch. Biochem. Biophys.* **410,** 1–6

69. Crompton, M. (1999) The mitochondrial permeability transition pore and its role in cell death. *Biochem. J.* **341,** 233–249

70. Panov, A. V., Andreeva, L., and Greenamyre, J. T. (2004) Quantitative evaluation of the effects of mitochondrial permeability transition pore modifiers on accumulation of calcium phosphate: comparison of rat liver and brain mitochondria. *Arch. Biochem. Biophys.* **424,** 44–52

71. Wyttenbach, A. (2004) Role of heat shock proteins during polyglutamine neurodegeneration: mechanisms and hypothesis. *J. Mol. Neurosci.* **23,** 69–96

72. Shinder, G. A., Lacourse, M. C., Minotti, S., and Durham, H. D. (2001) Mutant Cu/Zn-superoxide dismutase proteins have altered solubility and interact with heat shock/stress proteins in models of amyotrophic lateral sclerosis. *J. Biol. Chem.* **276,** 12791–12796

73. Sittler, A., Lurz, R., Lueder, G., Priller, J., Lehrach, H., Hayer-Hartl, M. K., Hartl, F. U., and Wanker, E. E. (2001) Geldanamycin activates a heat shock response and inhibits huntingtin aggregation in a cell culture model of Huntington's disease. *Hum. Mol. Genet.* **10,** 1307–1315

74. Kieran, D., Kalmar, B., Dick, J. R., Riddoch-Contreras, J., Burnstock, G., and Greensmith, L. (2004) Treatment with arimoclomol, a coinducer of heat shock proteins, delays disease progression in ALS mice. *Nat. Med.* **10,** 402–405